

# ESTIMATING PHENOLOGY OF AGRICULTURAL CROPS FROM SPACE

Juan M. Lopez-Sanchez<sup>1</sup>, Fernando Vicente-Guijalba<sup>1</sup>, J. David Ballester-Berman<sup>1</sup>, and Shane R. Cloude<sup>2</sup>

<sup>1</sup>Signals, Systems and Telecommunications Group, (SST, IUII), University of Alicante, P.O. Box 99, 03080 Alicante, Spain.  
E-mail: [juanma-lopez@ieee.org](mailto:juanma-lopez@ieee.org), [fernando.vicente@ua.es](mailto:fernando.vicente@ua.es), [davidb@ua.es](mailto:davidb@ua.es)

<sup>2</sup>AEL Consultants, 26 Westfield Avenue, Cupar, Fife, KY15 5AA, Scotland, UK. E-mail: [aclc@mac.com](mailto:aclc@mac.com)

## ABSTRACT

This paper summarises the main results derived from a study developed under the ESA funded PolSAR-Ap project, aimed to demonstrate the contribution of SAR polarimetry in diverse Earth observation products. The specific application treated here is the retrieval of phenology of agricultural crops by exploiting C-band polarimetric images. Using a set of 20 images acquired by Radarsat-2 during the AgriSAR2009 campaign, we show the sensitivity of polarimetry for some crop types (mainly cereals) and present a number of retrieval results with simple algorithms that exhibit excellent performance for some crops, e.g. barley and wheat.

## 1. INTRODUCTION

All agricultural crops present a continuous development, from sowing or transplanting to harvest, in which they grow and evolve in accordance with their biophysical characteristics and the farming practices applied to them. Phenology denotes such a succession of stages during the cultivation cycle, and is commonly expressed using numerical scales [1].

Tracking phenology of agricultural fields by remote sensing is useful for farmers with extensive fields because it provides key information for planning and triggering cultivation practices, so the main application of this Earth observation product is precision farming. These cultivation practices (e.g. irrigation, fertilisation, effective germination counting, harvest, etc.) require timely inputs about the status of the plants and, specifically, about their condition or situation along the cultivation cycle.

Besides precision farming, timely information of phenology can contribute to agencies and institutions involved in market predictions, insurance policies, subsidies claims, etc. since such information complements their own data sources and provides a temporal schedule for the crop production and yield calendar.

Most of the applications require phenology information at parcel (field) level, but in some cases it may be nec-

essary to provide values at pixel (sub-parcel) level, especially when dealing with detection of heterogeneities produced by cultivation problems (e.g. water salinity used of irrigation) and plant diseases (e.g. pests and plagues).

Phenology monitoring by satellite remote sensing has not attracted much attention in the past, due to the following two causes:

- Lack of time series of images (in the best cases there were data sets with large sampling intervals, e.g. 35 days for ERS and Envisat), which impeded the elaboration of timely information as would be required by end-users of such a product.
- Cost of the ground campaigns required to support the development of such algorithms, since they have to last as the cultivation cycle (e.g. 2 to 5 months), with frequent ground acquisitions over wide areas.

Fortunately, this situation has changed in the last dates, thanks to the launch of satellites with shorter revisit times (e.g. 11 days for TerraSAR-X) and reconfigurable acquisitions (different beams can be operated for more frequent observation of a particular area).

Algorithms for phenology monitoring have to be devised individually for each crop type, based on the expected response of each crop to the sensor at its different stages, which can be extracted from the data themselves (training sets) or from previous experiments, models and simulations. Recent examples of this methodology have been applied to rice fields, both at X-band [2] and C-band [3].

The starting point of this application is the knowledge of which crop type or plant species is cultivated at the monitored fields, which is provided by the users or can be obtained from a crop type map. Then, the general objective of this product consists in estimating the current phenological stage of the plants in the parcel by exploiting a single PolSAR acquisition.

## 2. METHODOLOGY

The problem of identifying the phenological stage of an agricultural crop can be regarded as a classification problem, where each stage corresponds to a class, and hence can be approached in a similar way to crop type mapping. This application is better suited to algorithms based on hierarchical trees or simple decision planes, since they can be tailored to match specifically the different features of the plants that change or appear as they develop. This type of rule-based algorithms facilitates the physical interpretation of the phenology retrieval procedure, since the criteria are based on scattering mechanisms (e.g. surface, dihedral, volume) and properties (e.g. extinction, depolarisation, etc.) in correspondence to the crop structure and features at each stage and in contrast with other algorithms based on the full covariance statistics (e.g. Wishart classifier). Hierarchical tree algorithms have been widely used for classification purposes in the literature, and specifically for crop-type mapping with PolSAR data, so they can be considered as mature since they provide consistently accuracies above 85% in crop type mapping. Therefore, hierarchical tree algorithms will be implemented and tested for this product.

The starting point is the multi-look processing or filtering of the available PolSAR images, providing the covariance or coherency matrix for each multi-looked pixel. A sliding boxcar filter has been employed since the monitored parcels are wide enough and homogeneous for applying such a filtering type. Then, all images have been geocoded. If all images were acquired with the same beam and pass, a coregistration of the whole set to a common master image could be used instead of geocoding. Once geocoded, all available PolSAR images are studied for each crop type by restricting the region of interest (ROI) to the interior of all fields of each crop. In all cases, an analysis of a large number of polarimetric observables is carried out in order to extract the most meaningful set for the crop under study. The available observables are backscatter powers and correlations (linear, Pauli, and circular basis, and for compact polarimetry as well), backscattering ratios for different channels and for various polarisation bases, eigenvector/eigenvalue decomposition parameters, compact polarimetry decomposition parameters, the Freeman-Durden and Touzi decomposition outputs.

This analysis is based on the representation of the observables as a function of phenology, so the reference data recorded at each acquisition date are used to define the x-axis of their representation. For each observable, the mean and standard deviation within the parcel at every radar acquisition are obtained and plotted.

From the analysis of the evolution of all observables for each crop type, a reduced set of them will be selected for the retrieval algorithm by identifying the ones that define with more distinction particular phenological stages. Specifically, those with wider dynamic ranges and less presence of ambiguities will be chosen. Moreover, ob-

servables with easy physical interpretations will be preferred to those with less clear explanations in terms of scattering physics. With the selected set of observables, a hierarchical tree is defined by setting manually thresholds based on the previous analysis.

An important question to address for the definition of the final product concerns the required spatial resolution since phenology can be provided either at pixel level (one value per multi-looked pixel) or at parcel level (one value per parcel). In the first case we could detect areas with different degrees of development within the same parcel, hence being also useful for localised farming practices such as irrigation and fertilisation. In the second case we would be interested in the global development of the crop field, which would be considered as homogeneous.

According to the available reference data (see Section 3), we know the phenology at several ground points of each field, but: 1) they are mostly coincident for the same parcel; and 2) available values are maximum and minimum values of phenological stages, instead of single values. Therefore, we have considered in the analysis that phenological data at each field and each date are the same for the whole field, being the mean the value adopted.

The inversion algorithm however has been applied both at pixel and parcel levels. This option increases the usefulness of the product for potential end-users since retrieved information is provided at different scales, i.e. at pixel level any possible heterogeneity within a field can be detected and, in addition, at parcel level an overall conclusion on the status of the field is obtained. For the estimation at parcel level, it will be computed as the mode of the estimates within the parcel in accordance with the available reference data.

## 3. GROUND DATA AND RADAR IMAGES

The test site for agriculture in this project is located in Indian Head, Canada (50°34'17" N, 103°36'36" W). Indian Head has been one of the three locations included in the ESA funded AgriSAR2009 campaign [4], together with Flevoland (The Netherlands) and Barrax (Spain). The amount and type of satellite radar data is similar in all three locations, but the ground campaign performed in Indian Head is the most complete and the only one including phenology records with fine time sampling and in numerical scale. The whole campaign took place from April to October 2009.

This site corresponds to an agricultural area in the Canadian prairies. Grain farming is predominant, but there is some mixed farming. Farms are managed with diverse crop rotations including cereal, oilseed and pulse crops.

The ground data collection was conducted in 2009 by the Indian Head Agriculture Research Facility (IHARF) and the University of Regina. Available ground data consist of two sets: an intensive detailed survey of representa-

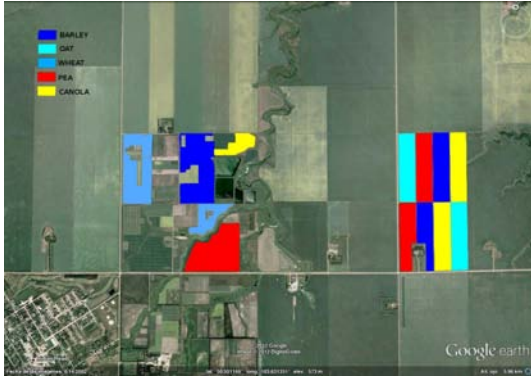


Figure 1. Location of the fields and crops employed in this study, overlaid on a GoogleEarth image.

tive crops in a small number of fields, and a more extensive but less detailed survey of crops over the entire test site. The intensive database, carried out between June and August 2009, is the one relevant for phenology monitoring, since data were acquired on a regular basis during 3 months with time sampling between 7 and 10 days. It comprises records gathered in 52 locations, of 14 different parcels, and a total of 6 different crop types: barley, oat, wheat, canola, field pea and flax.

Each point record has the following attributes: crop type and UTM coordinates, growth stage or phenology (multiple dates), NDVI (multiple dates), LAI (multiple dates), photos (multiple dates), and grain yield. Besides all these measurements daily meteorology information was acquired during the whole campaign from the Environment Canada weather station at Indian Head: temperature, humidity, rainfall, and wind.

From the original 6 crop types monitored in the intensive campaign, phenological information about the flax field was not provided in typical numerical scales, so the experiment is concentrated on the remaining 5 crop types. Figure 1 shows the location of the different fields and crops over a GoogleEarth image.

The available phenological information of the cereals (barley, oat and wheat) corresponds to the scale defined in [5], coincident with the standard BBCH scale [1], ranging from 0 to 100 in a continuous way. The phenological scales of canola and field pea are defined differently, so a redefinition was required to obtain a continuous scale.

Phenological information recorded during the ground campaign at each single point and date comprises a range of observed phenological stages, i.e. minimum and maximum, since when crops develop one can find at any time plants at different growth levels. This inherent uncertainty is considered in the BBCH standard by stating that the phenological stage of a field or parcel is defined as the value already reached by the 50% or more of the parcel area. However, that convention was not used in this campaign. Consequently, at each date we can know only the extreme phenologies present in the field, but not the dominant or average one. Figure 2 shows in a graph the

Table 1. Set of Radarsat-2 images

Date (yyyymmdd)	Pass	Beam	Inc. angle (deg)
20090603	Desc.	FQ02	22
20090604	Asc.	FQ19	39
20090611	Asc.	FQ15	35
20090617	Desc.	FQ10	30
20090624	Desc.	FQ14	34
20090701	Desc.	FQ19	39
20090702	Asc.	FQ02	22
20090704	Desc.	FQ06	26
20090711	Desc.	FQ10	30
20090712	Asc.	FQ11	31
20090721	Desc.	FQ02	22
20090722	Asc.	FQ19	39
20090726	Asc.	FQ02	22
20090804	Desc.	FQ10	30
20090811	Desc.	FQ14	34
20090812	Asc.	FQ06	26
20090818	Desc.	FQ19	39
20090819	Asc.	FQ02	22
20090822	Asc.	FQ15	35
20090829	Asc.	FQ11	31

recorded phenology for all crop types, together with the radar acquisitions. Note that for each crop type all fields grew quite similarly, so a single record can be assigned to each crop type without requiring processing differently the different fields of each crop.

The whole radar dataset is composed by 57 quad-pol Radarsat-2 images, acquired in 2009 from April 6 to September 28, all in fine-quad mode, with incidence angles ranging from  $20^\circ$  to  $40^\circ$ , in both ascending and descending passes. Each combination of beam (incidence angle) and ascending or descending pass constitutes a time series of 5 to 8 images, and there are 10 of such time series. From the whole set of 57 images, only those acquired between June 1st and August 31st were considered, since there is not phenological information for the rest of dates of the campaign. In addition, those images acquired in rainy conditions (more than 1 mm on the acquisition date) were discarded to avoid non modelled fluctuations and other artefacts. Consequently, the analysis was restricted to 20 valid images, corresponding to all beams and incidence angles (see details in Table 1).

## 4. RESULTS WITH FULLY POLARIMETRIC DATA AND VALIDATION

### 4.1. Analysis

First we describe and justify the evolution as a function of phenology of different parameters. To this end, all parameters presenting similar evolutions are grouped. In general, from the five crop types analysed (barley, oat, wheat, field peas and canola) we have found only three

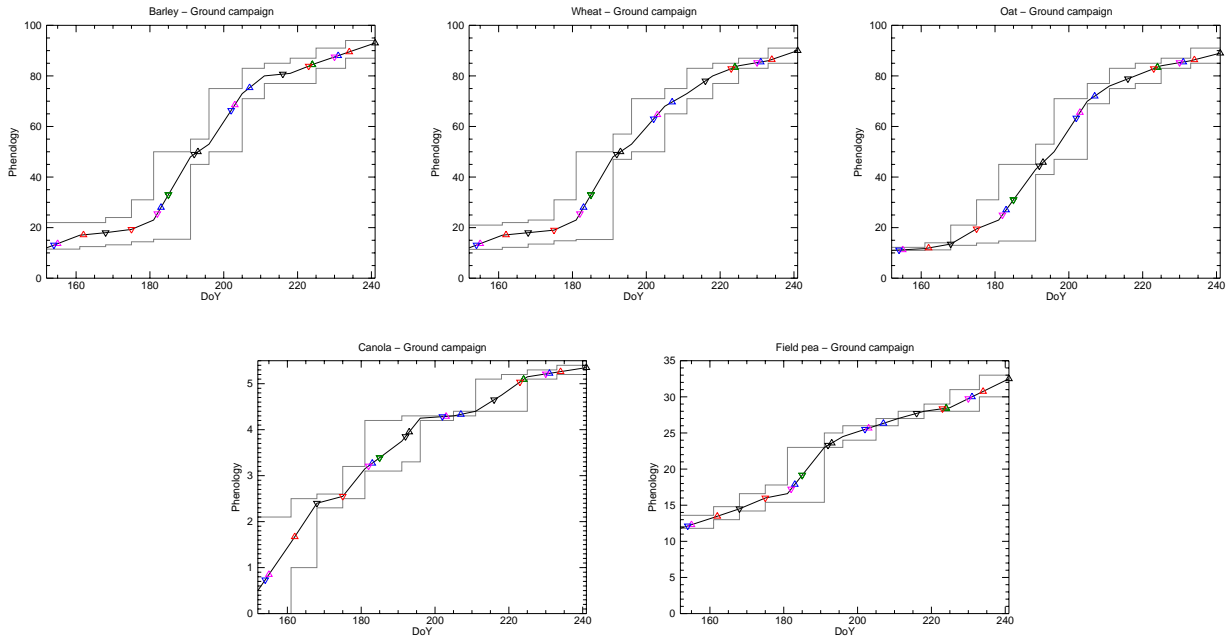


Figure 2. Graphical representation of the reference phenological data as a function of date (day of year, DoY) as recorded during the ground campaign. Gray lines denote the minimum and maximum values of phenology that could be found at each parcel and date. Black line results from interpolating the mean phenology at each ground acquisition date. Triangles indicate the presence of a radar image effectively acquired on that date. Triangles pointing up (down) denote ascending (descending) mode. Triangle colour indicates the incidence angle: blue at  $22^\circ$ , green at  $26^\circ$ , black at  $30-31^\circ$ , red at  $34-35^\circ$ , and magenta at  $39^\circ$ .

main signatures, since all three cereals (barley, oat and wheat) behave similarly.

Although in principle we expected clear differences in the radar responses as a function of incidence angle (there are images acquired with angles from 22 to 39 degrees), such differences are only evident in some parameters and especially for certain crop conditions (e.g. during the vegetative phase in cereals, since ground dominates the radar response). Consequently, a joint analysis of all angles has been carried out. In some extreme situations, like two images acquired on consecutive days with 22 and 39 degrees, a discontinuity is expected, so this will be commented when necessary.

Finally, and according to the discussion in the previous sections, we have computed the evolutions of all parameters at pixel level after a  $9 \times 9$  multi-look. The plots of the evolutions show the average and the standard deviation computed over the whole field.

In this report we will focus our analysis on the results on cereals (which benefit most strongly from polarimetry) and some additional short comments will be given on canola and pea fields. Only observables with some trends or sensitivity to phenology will be commented for each crop type. For instance, the evolution of three different observables as a function of phenology for all cereals results is shown in Fig. 3.

#### 4.1.1 Cereals

Parameters with high sensitivity:

- Linear crosspolar backscatter (HV) presents an increase both at the early stages (6-10 dB from stages 10 to 25-30) and the late ones (4-5 dB from stage 75), being quite constant in the middle (see Fig. 3). Similar parameters are HH-VV, RR and LL backscatter, and  $p_V$  of Freeman decomposition. Note that the increase in late stages is not present for oat (but at one single acquisition at  $22^\circ$ ).
- HHVV correlation decreases clearly during the vegetative phase (stages 10 to 50), and then remains around 0.4 with important differences between acquisitions. Similar parameters:
  - Average alpha increases from 0 to 45 degrees only during the vegetative phase.
  - RL/RR and RL/LL ratios show a decrease of 10 dB during the vegetative phase.
  - Correlations RRRL and LLRL behave similarly, especially for wheat.
- Entropy shows a sudden increase from 0.2 at stage 10 to 0.7-0.8 at stages 20-30, and then it remains around 0.8 all the time.

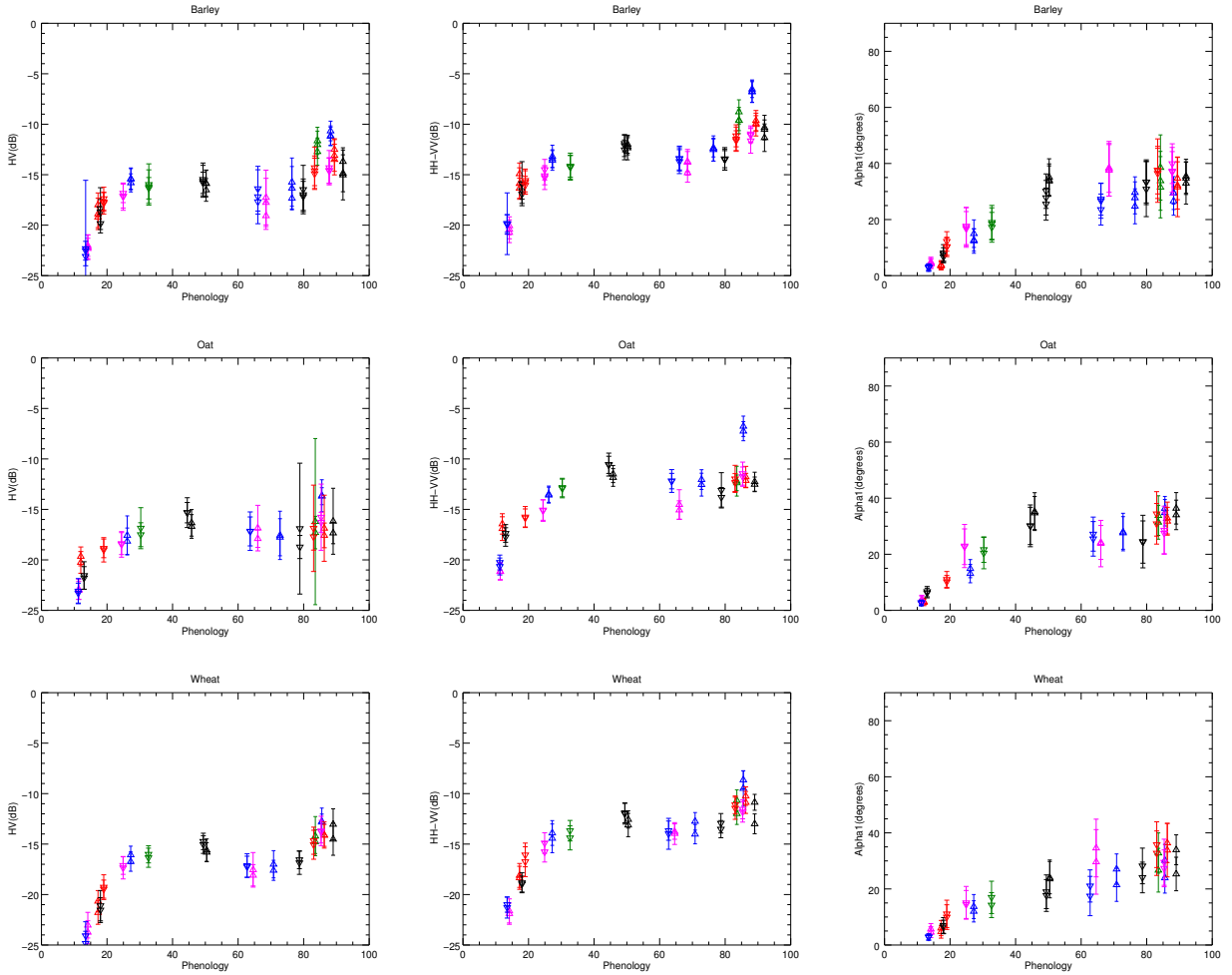


Figure 3. Evolution of  $HV$  ( $t_{33}$ ),  $HH-VV$  ( $t_{22}$ ) and dominant alpha ( $\alpha_1$ ) as a function of phenology for barley (top row), oat (middle row) and wheat (bottom row).

- Dominant alpha ( $\alpha_1$ ) increases monotonically during the whole cycle, but it is slightly saturated after the vegetative phase (see Fig. 3).
- Tau of Touzi decomposition is always close to zero, so the corresponding dominant alpha is like  $\alpha_1$  from the conventional eigenanalysis.

#### 4.1.2 Canola

The most remarkable result in this case is that the cross-polar backscatter follows a clear monotonic increasing trend for the whole growth period. This enables the phenology estimation in a straightforward way by using one single channel, HV. Indeed, coherent polarimetry does not contribute much to this crop type.

#### 4.1.3 Field pea

In general we found that many observables here are symmetrical with respect to stage 20-25, hence making it difficult to break the ambiguity between early and late stages

without any auxiliary information (e.g. time coordinate). Plants are always very short, so there is not much development or clear changes in terms of structure.

#### 4.2. Retrieval algorithms

In the following, details on the retrieval algorithm for cereals are given. After a close inspection of Fig. 3, a feasible algorithm could be designed to distinguish 4 different phenological intervals, i.e. early vegetative (stages 0-19), advanced vegetative (stages 20-39 or 20-44), late vegetative, reproductive and early maturation (stages from 40 or 45 to 79), and, finally, maturation (stages 80+).

The physical description of each interval is the following:

1. Surface scattering dominates the radar echo: very low entropy, alpha and  $\alpha_1$  close to zero, very low HV, high correlation between HH and VV.

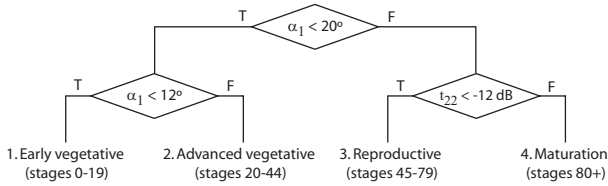


Figure 4. Basic hierarchical tree algorithm for cereals.  $t_{22}$  can be equivalently substituted by  $t_{33}$  setting the threshold in  $-15$  dB.

2. Vegetation starts to be present in the radar response, hence increasing entropy. Dominant alpha ( $\alpha_1$ ) is low (less than 20 degrees), but average alpha has already reached 40 degrees. Backscatter power will remain quite constant at all channels during this stage and the next one.
3. This corresponds to a moment of fast development in terms of phenology (buds, flowers, etc.), but not much change in terms of structure and, thus, radar response at least at C-band. Backscatter powers remain constant and both average alpha and  $\alpha_1$  too.
4. Finally, backscatter power increases at HV and HH-VV channels as a result of an increase of the randomness of the structure of the plants (but for oat, which remains as in previous stages since its morphology does not change).

A basic hierarchical tree algorithm can be defined in terms of just two parameters: dominant alpha angle ( $\alpha_1$ ) and backscatter power at HV or HH-VV ( $t_{33}$  or  $t_{22}$  entries of the coherency matrix). The proposed algorithm is depicted in Fig. 4.

### 4.3. Validation

The results obtained by applying the algorithm proposed in the previous section are analysed here for each crop type separately. As mentioned above, we will concentrate in cereals, where the benefits of polarimetry are well evident. An image showing the output of the retrieval algorithm applied at pixel level for wheat fields and for the 20 images is presented in Fig. 5. The statistics of the retrieved values and their comparison against the reference data is also shown in form of a table in Fig. 6. Results on oat and barley are summarised in the text.

#### 4.3.1 Wheat

Figures 5 and 6 show the retrieved results for wheat. We can appreciate how the most frequent phenology value at each data is in perfect agreement with the reference data at all dates but for one image acquired on July 2 (with 22 degrees incidence). This acquisition corresponds to an extreme incidence angle, so the proposed algorithm (common for all incidences) is more likely to fail. Nevertheless, the first images provide a 100% of pixels with the

right value. In later acquisitions, the transitions between successive stages are, in general, quite smooth in terms of the amount of pixels estimated to be at each stage around the transitions.

For some images there is a non negligible amount of pixels (more than 25%) assigned to wrong stages. These cases correspond to either dates of transition between successive stages or cases where the particular incidence angle affects more clearly the radar response. Anyway, the overall result demonstrates that the proposed algorithm is quite reliable despite its simplicity and it provides right estimates for 19 of the 20 images.

#### 4.3.2 Oat

Results for oat (not shown here) are not as good as for wheat after the early vegetative phase. In this case, the radar response does not change significantly from the 6th acquisition date onwards. Consequently, it is virtually impossible to distinguish the two last intervals, from stage 45 to the end of the season, and also separating the advance vegetative (interval 2) from the later stages.

With the proposed approach, the most frequent value of retrieved phenology from the 6th to the last image corresponds to interval 3 but in five of the images, hence demonstrating the lack of sensitivity for this crop type. The overall validation provides 13 right estimates at parcel scale from the 20 cases.

Attending at the physical characteristics of oat, the vegetation volume it is less dense and tall than other cereals (e.g. wheat and barley), so the radar response does not exhibit clear variations after the end of the vegetative phase and, moreover, the ground contribution is more present than for other cereals.

#### 4.3.3 Barley

The overall performance of the proposed algorithm for barley (tables not shown here) is quite similar to that of wheat, so the same comments apply. In this case the algorithm provides right estimates in all 20 images.

## 5. COMPARISON WITH SINGLE/DUAL POLARIMETRIC DATA

The analysis of the evolutions of radar observables as a function of phenology suggests that the dimensionality of the polarimetric space influences the number of different stages that could be identified for each crop type. As in the previous lines, the following analysis is focused on cereals since in this case polarimetry does play a substantial role for monitoring purposes.

For single polarisation, HH and VV exhibit low sensitivity to phenology and large dependence on incidence angle and even on ascending/descending mode (probably due to row orientation w.r.t. radar) in early stages. HV

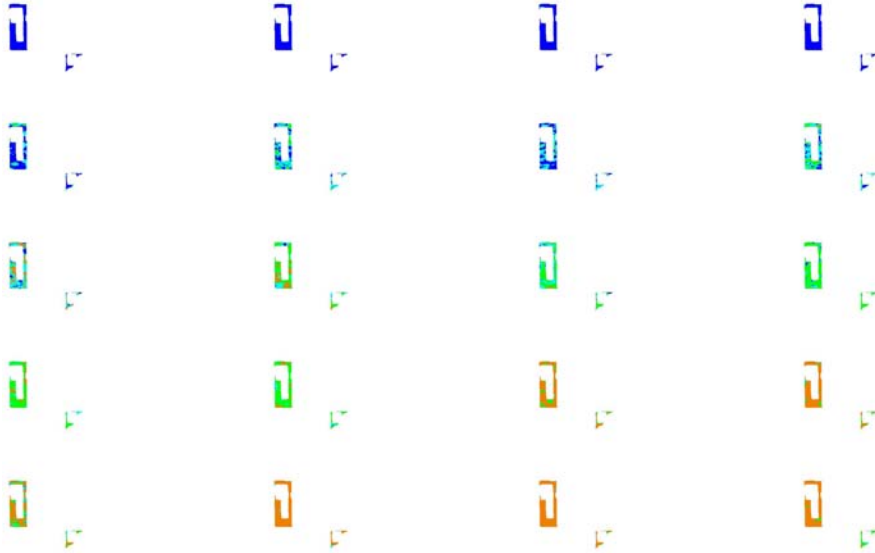


Figure 5. Results obtained for wheat: Map with the retrieved values at pixel level, formed by tiling the results corresponding to the 20 geocoded Radarsat-2 images considered in the study, ordered by acquisition date (ascending dates from left to right and top to bottom).

shows three stages in its evolution as a function of phenology, i.e. initial fast increase at early vegetative, slow decrease at central part from 20 to 80 stages, and late fast increase. Therefore, the number of stages to be separated is smaller than with full-pol, and there is more uncertainty between stages 10-20 and 20+. Moreover, the same threshold would not fit equally all cereals and should be adapted to each type.

In case of dual-pol, and provided the mentioned lack of sensitivity of HH and VV, typical dual-pol systems gathering HHVH or VVHV data do not show a clear improvement with respect to HV. Anyway, the joint use of HV and any of the HV/VV or HV/VV ratios provides enough information for barley and wheat to classify correctly the phenology for the three intervals mentioned in the previous paragraph (i.e. stages below 20, from 20 to 80, and above 80). Intermediate stages, however, are not separable in this observation space.

A HHVV coherent measurement, instead, provides similar performance to full-pol, since  $\alpha_1$  is quite similar to the  $\alpha_1$  gathered with full polarimetry and HH-VV is already used by the proposed algorithm. Anyway, such acquisitions suffer the same drawback of full polarimetry in terms of spatial coverage, due to the reduced swath required by doubling the PRF of the radar system.

Compact polarimetry [6, 7, 8] is expected to offer a slightly lower performance than full polarimetry but with a wider swath capability may suffice in some applications. Note that  $t_{33}$ ,  $t_{22}$  and  $\alpha_1$ , used for cereals in this study, are mapped approximately in an equivalent way by compact-pol using  $p_V$ ,  $p_D$ , and  $\alpha_s$ .

## 6. CONCLUSIONS

Table 2 summarises the useful parameters for each crop type according to the retrieval results presented previously. We confirm that the sensitivity of C-band polarimetry to crop phenology is defined by the presence of different morphologies of plants and parcels as they develop along the cultivation cycle.

For cereals with distinct plant structures at different stages, polarimetry enables the estimation of their growth stage (from a set of 4 significant intervals) by exploiting just a single radar acquisition, without any other additional information. It is also pointed out that the use of time coordinate, enabled by the availability of time series of radar data from current SAR sensors, will definitely improve the estimation accuracy even more.

The conclusions from this study can be extrapolated to other crop types by taking into account the physical rationale employed to establish the retrieval algorithms. Hence, phenology is likely to be retrieved for every crop with development features analogous to those analysed here. In addition, the wide range of incidence angles employed in this study, despite their influence in the observables, demonstrates the robustness of this application.

According to the most important observables found in this study ( $t_{33}$ ,  $t_{22}$  and  $\alpha_1$ ), a compact-pol sensor would be able to provide most of the polarimetric sensitivity required for this application and wide swath coverage. It is noted that only in case of canola fields, because of its particular morphology, dual-pol and single-pol systems would suffice.

WHEAT		RESULTS: Percentage of pixels				GROUND DATA	
Date – Acquisition	Total pixels	1	2	3	4	Original	Acq. Date
20090603.rds2_DSC/22deg	4918	100	0	0	0	11.6-12.3	20090601
20090604.rds2_ASC/39deg	4918	100	0	0	0		
20090611.rds2_ASC/35deg	4918	99,17	0,83	0	0	13.0-13.5, 20-22	20090610
20090617.rds2_DSC/30deg	4918	98,64	1,36	0,00	0,00	13.7-14.4, 20-22	20090617
20090624.rds2_DSC/34deg	4918	68,00	26,35	5,65	0,00	14.7-15.6, 20-24	20090624
20090701.rds2_DSC/39deg	4918	29,69	52,50	17,81	0,00	15.5-16.5, 21-24, 31	20090630
20090702.rds2_ASC/22deg	4918	50,22	46,22	3,13	0,43		
20090704.rds2_DSC/26deg	4918	22,61	51,83	23,95	1,61		
20090711.rds2_DSC/30deg	4918	13,26	52,97	7,65	26,13	45-50	20090708
20090712.rds2_ASC/31deg	4918	2,14	20,37	52,03	25,46		
20090721.rds2_DSC/22deg	4918	4,49	36,82	56,41	2,28	50-55	20090715
20090722.rds2_ASC/39deg	4918	4,43	14,82	80,56	0,18		
20090726.rds2_ASC/22deg	4918	0,12	10,00	77,63	12,24	71-75	20090724
20090804.rds2_DSC/30deg	4918	0,53	9,64	78,63	11,20	77-83	20090730
20090811.rds2_DSC/34deg	4918	0,00	1,14	17,87	80,99	83-85	20090806
20090812.rds2_ASC/26deg	4918	0,16	2,05	9,56	88,23		
20090818.rds2_DSC/39deg	4918	1,59	11,08	27,25	60,09	83-87	20090813
20090819.rds2_ASC/22deg	4918	0,00	2,72	0,00	97,28		
20090822.rds2_ASC/35deg	4918	0,00	1,26	1,30	97,44	87-91	20090821
20090829.rds2_ASC/31deg	4918	0,02	1,32	12,71	85,95	92-94	20090829

Figure 6. Results obtained for wheat: Percentage of pixels assigned to each stage at each image and available reference data. The most frequent value at each date is coloured according to the scale employed in the map.

Table 2. Summary of useful parameters for each crop type

Crop type	Parameters
Cereals	$\alpha_1$ , HH-VV ( $t_{22}$ ), HV ( $t_{33}$ ), $p_V$ (Freeman), RR, LL, RL/RR, RL/LL, correlations: HHVV, RRRL and LLRL
Canola	HH-VV ( $t_{22}$ ), HV ( $t_{33}$ ), $p_V$ (Freeman), RR, LL
Pea	HH-VV ( $t_{22}$ ), Std.Dev. of RR, HHVV correlation, entropy, average alpha, $p_V$ (Freeman), RR, LL, RL/LL, RL/RR

## ACKNOWLEDGEMENTS

This work has been developed in the framework of project PoISAR-Ap (AO 1-6707/11/I/NB) funded by ESA. It is also supported by the Spanish Ministry of Economy and Competitiveness (MINECO) and EU FEDER under Project TEC2011-28201-C02-02.

All Radarsat-2 images have been provided by MDA and CSA in the framework of the ESA funded AgriSAR2009 campaign. RADARSAT-2 Data and Products ©MacDonald, Dettwiler and Associates Ltd. (2009) – All Rights Reserved. RADARSAT is an official trademark of the Canadian Space Agency. Ground measurements were acquired by AAFC and IHARF.

## REFERENCES

- U. Meier, Ed., *Growth Stages of Mono- and Dicotyledonous Plants. BBCH Monograph*, 2nd edition, 2001.
- J. M. Lopez-Sanchez, S. R. Cloude, and J. D. Ballester-Berman, “Rice phenology monitoring by means of SAR polarimetry at X-band,” *IEEE Trans. Geosci. Remote Sensing*, vol. 50, no. 7, pp. 2695–2709, July 2012.
- J. M. Lopez-Sanchez, F. Vicente-Guijalba, J. D. Ballester-Berman, and S. R. Cloude, “Polarimetric response of rice fields at C-band: Analysis and phenol-

ogy retrieval,” *IEEE Trans. Geosci. Remote Sensing*, 2013, In press.

- R. Caves et al., “AgriSAR2009 Final Report, Vol. 1. Executive Summary, Data Acquisition, Data Simulation,” Tech. Rep., 2011, Available online: <http://earth.esa.int/campaigns/>.
- J. C. Zadoks, T. T. Chang, and C. F. Konzak, “A decimal code for the growth stages of cereals,” *Weed Research*, vol. 14, no. 6, pp. 415–421, Dec. 1974.
- F. J. Charbonneau et al., “Compact polarimetry overview and applications assessment,” *Can. J. Remote Sensing*, vol. 36, no. 2, 2010.
- J. D. Ballester-Berman and J. M. Lopez-Sanchez, “Time series of hybrid-polarity parameters over agricultural crops,” *IEEE Geosci. Remote Sensing Letters*, vol. 9, no. 1, pp. 139–143, Jan. 2012.
- S. R. Cloude, D. G. Goodenough, and H. Chen, “Compact decomposition theory,” *IEEE Geosci. Remote Sensing Letters*, vol. 9, no. 1, pp. 28–32, Jan. 2012.